



DISCLAIMER

This report has been prepared by the Institute of Geological and Nuclear Sciences Limited (GNS Science) exclusively for and under contract to EQC. Unless otherwise agreed in writing by GNS Science, GNS Science accepts no responsibility for any use of, or reliance on, any contents of this report by any person other than EQC and shall not be liable to any person other than EQC, on any ground, for any loss, damage or expense arising from such use or reliance.

The data presented in this report are available to GNS Science for other use from November 2014.

BIBLIOGRAPHIC REFERENCE

Holden, C. 2014. Ground motion modelling of an Alpine fault earthquake and a Hope fault earthquake for main South Island cities (NZ), *GNS Science Consultancy Report 2014/257*. 24 p.

CONTENTS

EXECUTIVE SUMMARY.....	IV
1.0 INTRODUCTION	1
2.0 METHOD	6
2.1 A CHARACTERIZED SOURCE MODEL	6
2.2 COMPUTING HYBRID SEISMOGRAMS.....	6
2.2.1 Stochastic approach for frequencies above 1Hz.....	7
2.2.2 Discrete wavenumber approach for frequencies lower than 1Hz	7
2.3 SITE EFFECTS.....	7
3.0 CHARACTERISING A LIKELY RUPTURE SCENARIOS ON THE ALPINE FAULT.....	9
3.1 OUTER PARAMETERS	9
3.2 INNER PARAMETERS.....	10
3.3 EXTRA PARAMETERS.....	11
4.0 CHARACTERISING A LIKELY RUPTURE SCENARIO ON THE HOPE FAULT	12
4.1 OUTER PARAMETERS	12
4.2 INNER PARAMETERS.....	13
4.3 EXTRA PARAMETERS.....	13
5.0 ACCELERATION TIME HISTORIES AND RESPONSE SPECTRA FROM AN ALPINE FAULT EARTHQUAKE	14
5.1 ACCELERATION TIME HISTORIES	14
5.2 RESPONSE SPECTRA.....	15
6.0 ACCELERATION TIME HISTORIES AND RESPONSE SPECTRA FROM A HOPE FAULT EARTHQUAKE	17
6.1 ACCELERATION TIME HISTORIES	17
6.2 RESPONSE SPECTRA.....	18
7.0 OUTCOMES OF THIS RESEARCH PROJECT	20
8.0 ACKNOWLEDGEMENTS.....	21
9.0 REFERENCES	22

FIGURES

Figure 1	Map of the South Island and active faults, and the three population centres selected for our study.....	2
Figure 2	Comparison between response spectra (5% damped) obtained from the McVerry et al. (2006) GMPE model (Site Class D) in green for a Mw 7.1 strike-slip event and the recorded response spectra (5% damped) from the 2010 Mw7.1 Darfield earthquake at two GeoNet strong motion stations, KOKS (dashed line) and CECS (continuous line), located at similar epicentral distances (112 and 120 km respectively) (see location on Figure 1).....	3
Figure 3	Map of the South Island showing principal features of the Australia–Pacific plate boundary, including the Alpine Fault, Puysegur subduction zone, and Marlborough fault system (Wairau, Awatere, Clarence and Hope faults).....	4
Figure 4	Location of the Hope Fault in the Marlborough Fault Zone (MFZ) (bold lines), Northern South Island.	5
Figure 5	Horizontal amplification function for Site Class D soil type (Kaiser et al., 2014) based on the average site amplification for Class D sites in Canterbury.....	8
Figure 6	Characterized source model for a Mw 8.2 Alpine fault rupture; the model consists of a background area (blue) of 500 by 18 km and 3 asperity areas of 50 by 10 km each.	10
Figure 7	Characterized source model for an Mw 7.1 Hope Fault rupture; the model consists of a background area (blue) of 45 by 13 km and 1 asperity of 12 by 10 km each.	13
Figure 8	Horizontal and vertical synthetic acceleration histories for rock sites as modelled from a Mw 8.2 Alpine fault earthquake in Greymouth, Hokitika and Christchurch (top to bottom).....	14
Figure 9	Horizontal and vertical synthetic acceleration histories for a Site Class D site as modelled from a Mw 8.2 Alpine fault earthquake in Greymouth, Hokitika and Christchurch (top to bottom).	15
Figure 10	Horizontal and vertical response spectra (5% damped) for rock sites (blue), Site Class D (red) soil sites as modelled from a Mw 8.2 Alpine Fault earthquake in Greymouth, Hokitika and Christchurch (top to bottom).	16
Figure 11	Horizontal and vertical synthetic acceleration histories for rock sites as modelled from a Mw 7.1 Hope fault earthquake in Greymouth, Hokitika and Christchurch	17
Figure 12	Horizontal and vertical synthetic acceleration histories for Site Class D soil sites as modelled from a Mw 7.1 Hope fault earthquake in Greymouth, Hokitika and Christchurch.....	18
Figure 13	Horizontal and vertical response spectra (5% damped factor) for rock sites (blue), Site Class D (red) soil sites as modelled from a Mw 7.1 Hope fault earthquake in Greymouth, Hokitika and Christchurch.....	19

TABLES

Table 1	Estimated closest distance (km) to the fault rupture of a potential Mw 8.2 Alpine earthquake and a Mw 7.1 Hope fault earthquake for the three selected sites in this study.	2
Table 2	Source characteristics of the main event and the 3 modelled asperities for an Mw 8.2 Alpine fault characterized source model.....	10
Table 3	Source characteristics of the main event and the modelled asperity for an Mw 7.1 Hope fault characterized source model.....	13
Table 4	Peak ground acceleration values from the broadband modelling in this study (left column) and the McVerry et al. (2006) model (GMPE) (right column) for an Alpine fault earthquake at selected locations.	15
Table 5	Peak ground acceleration values from broadband modelling in this study (left column) and the McVerry et al. (2006) model (GMPE) (right column) for a Hope Fault earthquake at selected locations.....	18

EXECUTIVE SUMMARY

The large September 2010 and the tragic February 2011 Canterbury earthquakes caused widespread damage by ground shaking and sand liquefaction in the Canterbury region. Both earthquakes were less than 50 km from the Christchurch central business area and had a magnitude that is much smaller than that expected from the Alpine Fault ($M_w=8.2$) and that is similar to a potential Hope Fault event (M_w7+). At present, the response spectra from a great scenario earthquake from the Alpine fault can only be estimated from ground-motion prediction equations (GMPEs) based on local and overseas earthquake records. A major problem of all GMPEs, including even the latest GMPEs from the next generation attenuation (NGA), for example, Abrahamson and Silva (2008), is their very large variability in ground motion predictions for large and great earthquakes.

Recent advances in earthquake mechanics allow us to compute seismograms for realistic earthquake scenarios, at specific locations, and with specific site conditions. Such simulations can provide very useful alternative estimates of possible ground motions from large faults for major population centres. In this study, instead of using GMPE, we carry out synthetic broadband simulations to derive synthetic strong-motion records.

The synthetic broadband strong-motion records are produced for both a possible large Alpine Fault earthquake ($M_w8.2$) and a large Hope Fault earthquake ($M_w7.1$) at sites in a number of selected population centres that may be strongly affected. The synthetic records show that ground motion accelerations in Greymouth and Hokitika are expected to exceed 20%g and 50%g respectively during an Alpine fault earthquake, while ground motions in Christchurch are expected to be moderate, with peak ground accelerations (PGAs) of 8%g expected from an Alpine event and 6%g from a Hope fault event.

Synthetic ground motions from the broadband simulations are generally consistent with PGAs estimated from GMPEs. However the modelled PGA from an Alpine Fault event in Hokitika is 59%g, twice the level expected from a GMPE for a PGA of 27%g. This high PGA is likely due not only to non-linear soil response not accounted for in this study but also to the presence of a modelled asperity nearby and to strong directivity effects, neither of which are accounted for in current GMPE modelling for New Zealand.

Response spectra are computed from the synthetic ground motions, and are compared to those estimated from the New Zealand GMPE. In general the response spectra from the simulations exceed the spectra derived from GMPE except for spectral periods between 0.5 and 1.2 seconds. The duration of shaking is expected to last over 3 minutes for an Alpine Fault earthquake and at least 20 seconds for a Hope fault earthquake. Such a duration is comparable to the duration observed in Christchurch from the 2010 M_w 7.1 Darfield earthquake.

LAYMAN ABSTRACT

The large September 2010 and the tragic February 2011 Canterbury earthquakes caused widespread damage by ground shaking and sand liquefaction in the Canterbury region. Both earthquakes were less than 50 km from the Christchurch central business area and had a magnitude that is much smaller than that expected from the Alpine Fault ($M_w=8.2$) and that is similar to a potential Hope Fault event (M_w7+). Response spectra are very useful tools for analysing the seismic performance of structures. At present, the response spectra from a great scenario earthquake from the Alpine fault can only be estimated from ground-motion prediction equations (GMPEs) based on local and overseas earthquake records. A major problem of all GMPEs, including even the latest GMPEs from the next generation attenuation (NGA), for example, Abrahamson and Silva (2008), is their very large variability in ground motion predictions for large and great earthquakes.

Recent advances in earthquake mechanics allow us to compute seismograms for realistic earthquake scenarios, at specific locations, and with specific site conditions. Such simulations can provide very useful alternative estimates of possible ground motions from large faults for major population centres. In this study, instead of using GMPE, we carry out synthetic broadband simulations to derive synthetic strong-motion records.

The synthetic broadband strong-motion records are produced for both a possible large Alpine Fault earthquake ($M_w8.2$) and a large Hope Fault earthquake ($M_w7.1$) at sites in a number of selected population centres that may be strongly affected. The synthetic records show that ground motion accelerations in Greymouth and Hokitika are expected to exceed 20%g and 50%g respectively during an Alpine fault earthquake, while ground motions in Christchurch are expected to be moderate, with peak ground accelerations (PGAs) of 8%g expected from an Alpine event and 6%g from a Hope fault event.

Synthetic ground motions from the broadband simulations are generally consistent with PGAs estimated from GMPEs. However the modelled PGA from an Alpine Fault event in Hokitika is 59%g, twice the level expected from a GMPE for a PGA of 27%g. This high PGA is likely due not only to non-linear soil response not accounted for in this study but also to the presence of a modelled asperity nearby and to strong directivity effects, neither of which are accounted for in current GMPE modelling for New Zealand.

Response spectra are computed from the synthetic ground motions, and are compared to those estimated from the New Zealand GMPE. In general the response spectra from the simulations exceed the spectra derived from GMPE except for spectral periods between 0.5 and 1.2 seconds. The duration of shaking is expected to last over 3 minutes for an Alpine Fault earthquake and at least 20 seconds for a Hope fault earthquake. Such a duration is comparable to the duration observed in Christchurch from the 2010 M_w 7.1 Darfield earthquake.

1.0 INTRODUCTION

In the design process for structures in New Zealand, strong motion records that have appropriate tectonic categories, focal mechanism, magnitude and distance ranges, and site conditions are selected and scaled to match the appropriate design spectra from the current New Zealand design code or the spectra from a probabilistic seismic hazard study. If the site for an engineering application is within 10 km of an active fault, forward directivity and fault fling effects are also important features for the selected strong-motion records. Even from a dataset of world-wide earthquakes, it is often not possible to select a set of strong-motion records with all the desired parameters. It is even more difficult to select an appropriate set of strong motion records from a great earthquake, such as a possible earthquake with a moment magnitude of 8.2 on the Alpine Fault in the South Island (Figure 1). For such a large earthquake, the location of asperities and the variation of slip along the fault, the duration of strong shaking, and the level of possible stress-drop are very important. However these parameters are not available in the attenuation models used in a seismic hazard analysis. The limited number of strong-motion records in the world-wide dataset means that few records can satisfy all the required conditions. Recent GNS Science research results (Zhao and Xu 2012; Zhao 2011) suggested that the variability of predicted response spectrum from different modern GMPEs for large crustal and subduction interface earthquakes is very large. The New Zealand GMPEs (McVerry et al., (2006) and Bradley (2013)) may not predict the response spectra from a Mw=8.2 Alpine Fault earthquake accurately. Figure 2 provides a simple comparison of response spectra (5% damped) obtained from the 2006 Mc Verry GMPE model (McVerry et al. 2006) for a Mw 7.1 strike-slip event and recorded response spectra (5% damped) from the 2010 Mw7.1 Darfield earthquake at GeoNet strong motion sites KOKS and CECS, located at similar epicentral distances (112 and 120 km respectively (Figure 1)). The recorded spectrum at KOKS (dashed line) matches very well the expected response spectrum level from the GMPE modelling. However the recorded response spectrum at CECS (continuous line) is clearly under-predicting ground motion spectral levels for periods between 0.5 and 1.5 seconds. This variability in response spectra clearly highlights the need to use broadband simulations for large events.

Recent advances in earthquake mechanics allow us to compute broadband seismograms for realistic earthquake scenarios, at specific locations, and with specific site conditions. We base our study on the Irikura and Miyake (2011) assumption that large accelerations are generated from asperities while the ground motions from the rest of the fault rupture area are negligible. The background slip makes up the total moment of the earthquake. The seismograms are calculated using a hybrid approach, and local site effects are modelled by using a frequency dependant site amplification function (Kaiser et al. 2013).

In this study we performed broadband simulations at 3 selected population centres (Christchurch, Greymouth and Hokitika) for a pair of potential large earthquakes in the South Island: an Mw 8.2 Alpine fault earthquake and an Mw 7.1 Hope fault event (Figure 1). The Alpine Fault is a major dextral-reverse fault that has produced large earthquakes (c. Mw=7.9) every 200–400 years with the last one in 1717 AD (Figure 3). The last rupture of the Hope Fault was in 1888 when an earthquake with an estimated moment magnitude of 7-7.3 produced fault slip of about 2.5 m in the horizontal direction (Figure 4). Our modelling of a Hope fault rupture is based on this event. Hokitika and Greymouth are major population centres that will be affected severely by future earthquakes from these faults, while Christchurch is a natural study site that has been subjected to strong shaking during the 2010-2011 Canterbury earthquake sequence (See Table 1 and Figure 1).

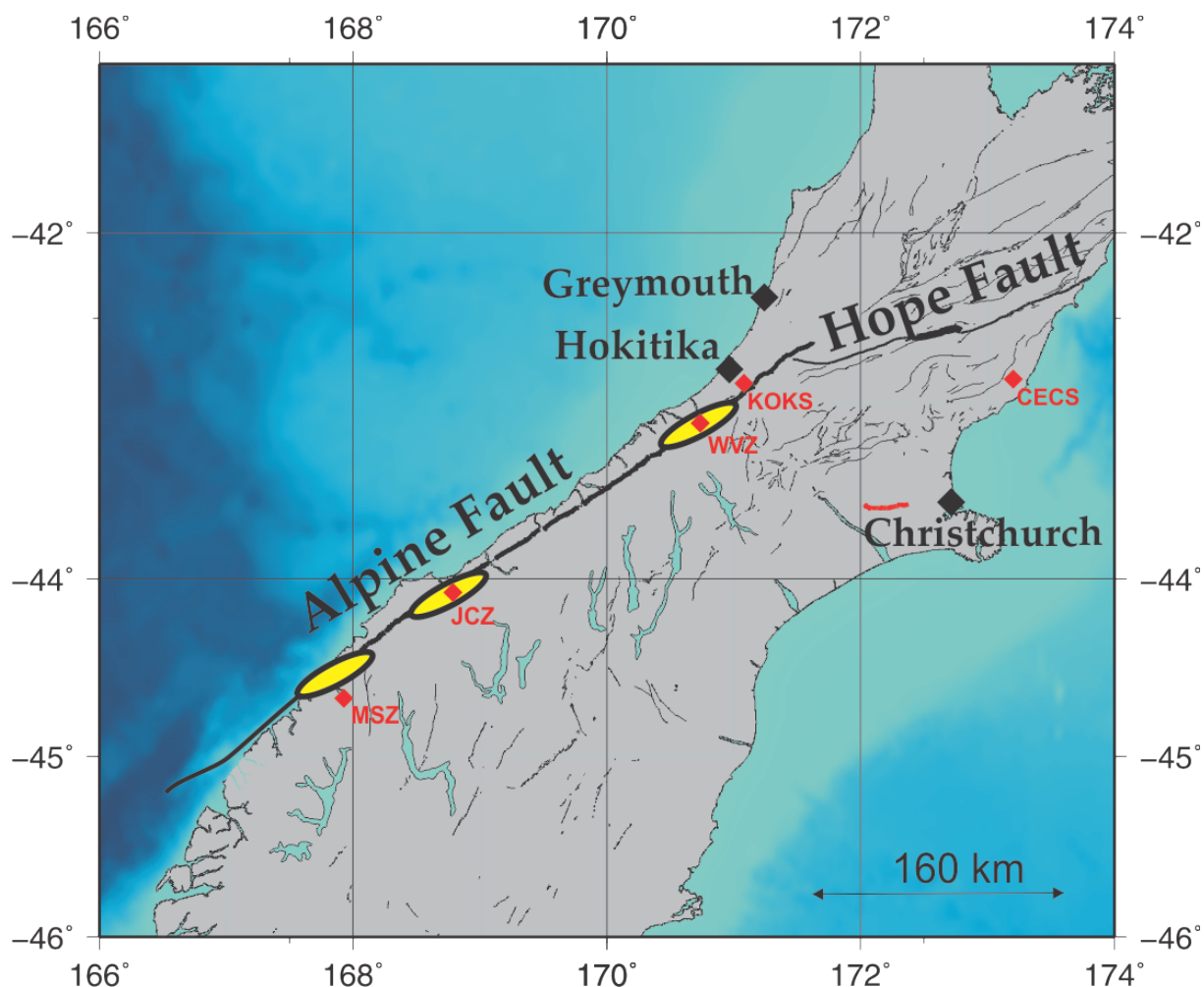


Figure 1 Map of the South Island and active faults, and the three population centres selected for our study. The bold line is the length of the likely Alpine Fault and Hope Fault (Hope River segment) ruptures; the red line is the fault trace from the Mw 7.1 Darfield earthquake. The yellow ellipses represent the major potential asperity locations proposed in this study. The red diamonds are locations of GeoNet strong motion stations mentioned in this study.

Table 1 Estimated closest distance (km) to the fault rupture of a potential Mw 8.2 Alpine earthquake and a Mw 7.1 Hope fault earthquake for the three selected sites in this study.

	Alpine fault	Hope fault
Greymouth	36	97
Hokitika	19	116
Christchurch	134	105

Firstly we detail the methods used to characterize the earthquake source, to compute the seismograms and to account for site effects. Then we present in detail the characterized source models for an Alpine rupture and a Hope Fault rupture. Finally we analyse the obtained synthetic seismograms and response spectra.

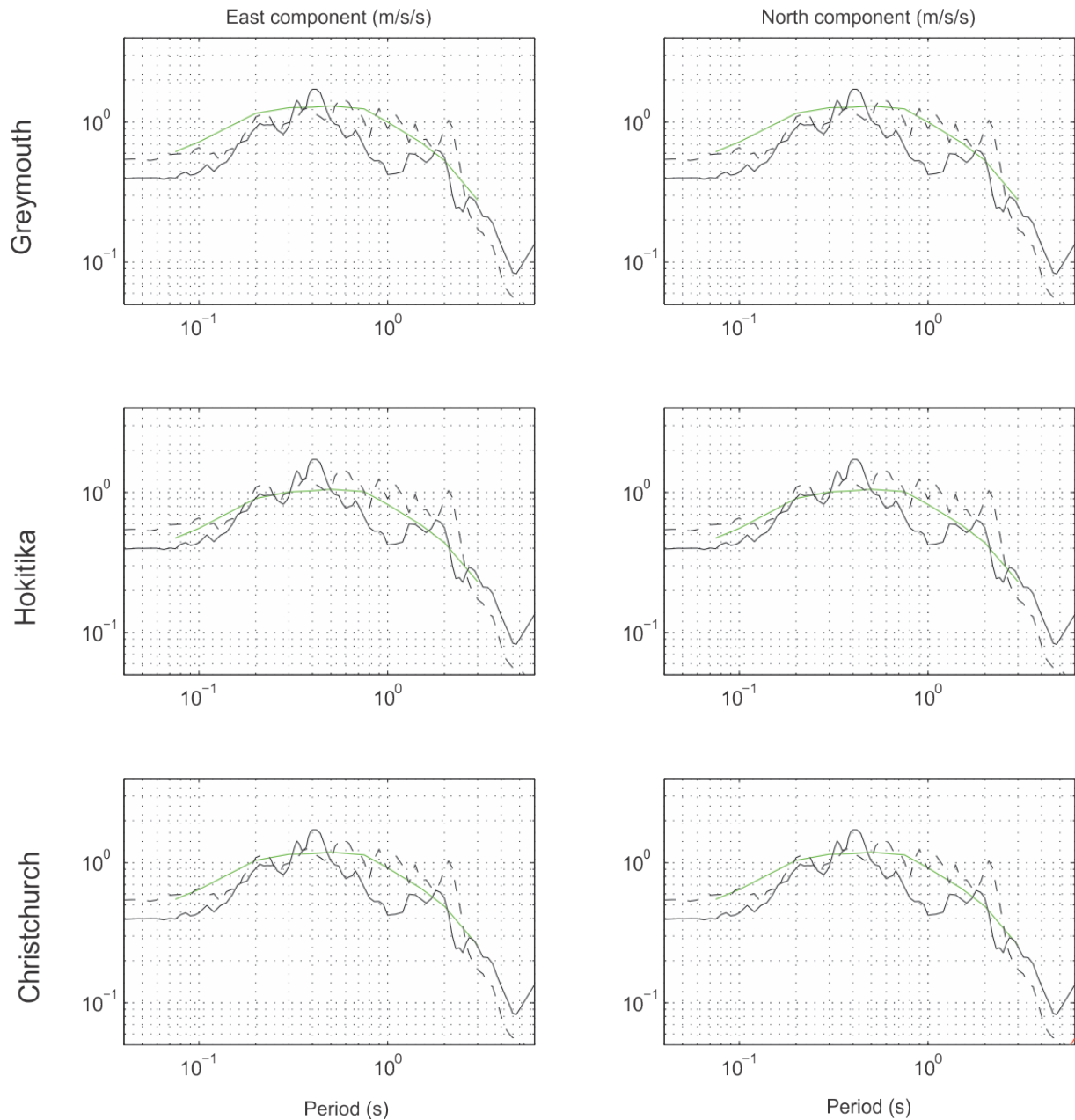


Figure 2 Comparison between response spectra (5% damped) obtained from the McVerry et al. (2006) GMPE model (Site Class D) in green for a Mw 7.1 strike-slip event and the recorded response spectra (5% damped) from the 2010 Mw7.1 Darfield earthquake at two GeoNet strong motion stations, KOKS (dashed line) and CECS (continuous line), located at similar epicentral distances (112 and 120 km respectively) (see location on Figure 1).

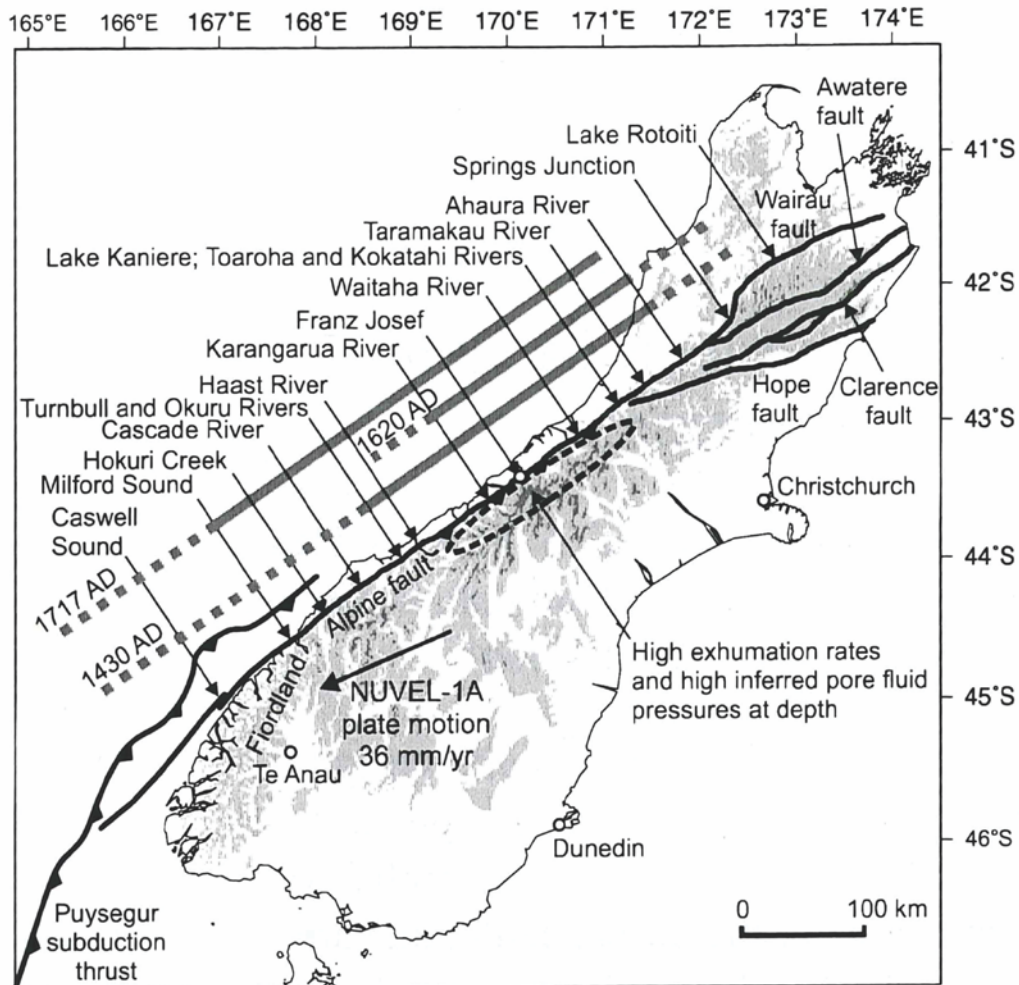


Figure 3 Map of the South Island showing principal features of the Australia–Pacific plate boundary, including the Alpine Fault, Puysegur subduction zone, and Marlborough fault system (Wairau, Awatere, Clarence and Hope faults). The thick grey lines indicate the inferred extent of past Alpine Fault ruptures. Grey shading demarcates topography higher than 800 m (from Sutherland et al. 2007).

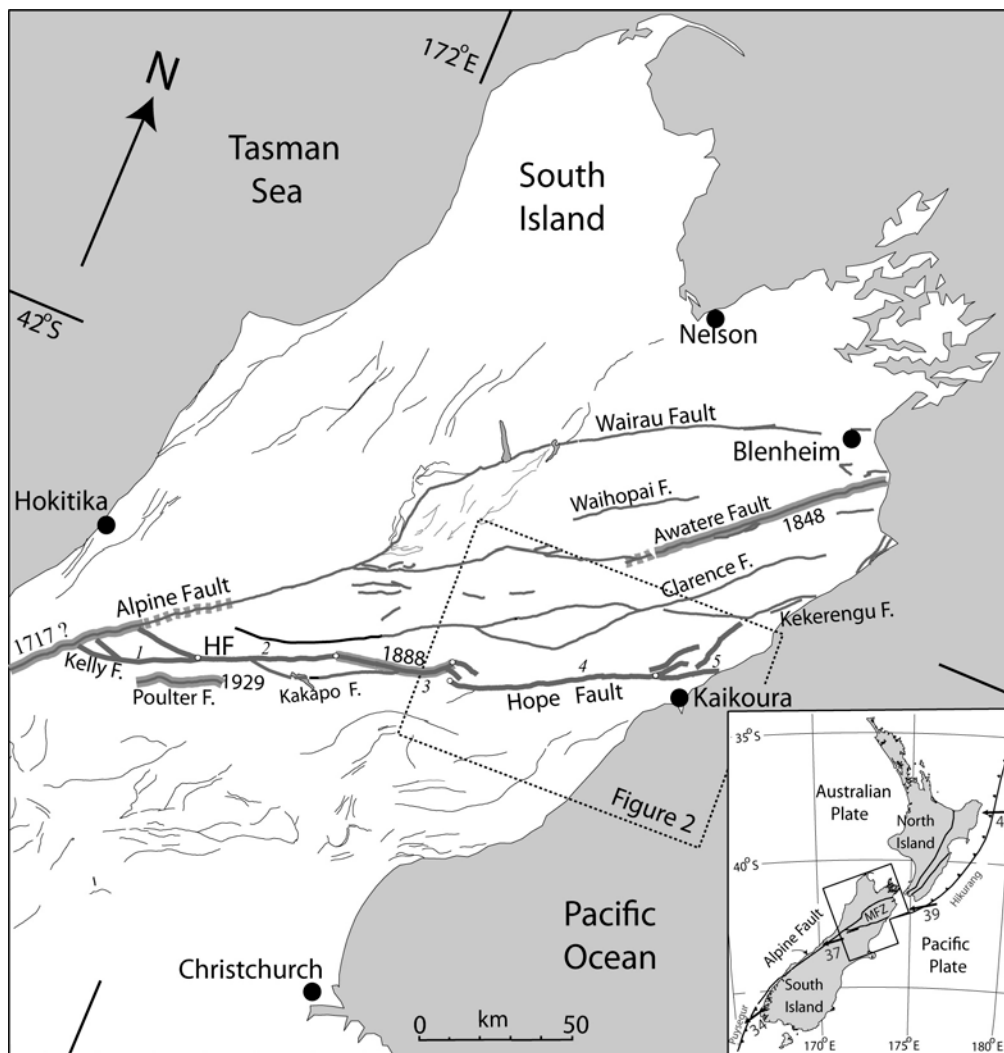


Figure 4 Location of the Hope Fault in the Marlborough Fault Zone (MFZ) (bold lines), Northern South Island. The Hope Fault System is shown boldest and fault segments are numbered in italics with segment 3 (Hope River Segment) being modelled in this study; segment boundaries being marked by open circles. Surface fault ruptures, e.g., 1888 North Canterbury earthquake, are shown as grey bands. Inset: New Zealand plate boundary including Alpine Fault, MFZ and Hikurangi Trough. Nuvel-1 directions (arrows) and plate rates relative to Australian Plate (in mm/yr) (adapted from Figure 1 in Langridge et al., 2003).

2.0 METHOD

There is a variety of methodologies available to calculate synthetic ground motions. The methodologies vary in the approach employed to characterise the earthquake source, in the method employed to compute the synthetics, and finally in the modelling of site effects. Examples of on-going research on ground motion modelling for earthquakes in New Zealand include purely stochastic approaches (Holden et al. 2014), physics-based hybrid approaches (Bradley and Graves, 2014; Benites and Olsen, 2010), high-frequency scattering theory (Mai et al., 2010) and dynamic fault modelling (Aagaard et al., 2012).

As we are particularly interested in broadband simulations of strong ground motion, we compute seismograms using a hybrid approach combining a simple discrete wavenumber approach and a stochastic method. The discrete wavenumber method is important to account for long periods and various phase arrivals. The stochastic method is particularly efficient for the high frequency part of the simulations (controlling peak accelerations). To define the earthquake sources, we apply the validated recipe based on a characterised source model for large crustal earthquakes developed by Irikura and Miyake (2011). The synthetic rock site motions are then used as the input motion for a frequency-dependant site amplification function.

2.1 A CHARACTERIZED SOURCE MODEL

Following the strong-motion prediction recipe, the sources are characterised by three types of parameters. Firstly, the outer parameters characterise the overall rupture, such as the seismic moment and the size and geometry of the fault plane. Secondly, the inner source parameters are related to heterogeneities on the fault plane. Finally, the extra source parameters characterise the kinematic aspects of the rupture such as the nucleation and termination location and time. The technique has proven very successful at computing ground motions for moderately large crustal events such as the Mw=6.9 1995 Kobe earthquake (Kamae et al. 1998), the Mw=6.8 2000 Tottori earthquake (Pulido et al. 2004) and very large crustal events such as the 2008 Mw 7.9 Wenchuan earthquake (Kurahashi and Irikura 2010). This technique has been recently applied to a very specific Alpine Fault rupture scenario (“worst-case” scenario) for a Christchurch location (Holden and Zhao 2011) in a preliminary study with many source parameters selected conservatively. In this study we compute ground motions at 3 selected population centres that are likely to be affected by such a large earthquake based on source parameters representing the most likely scenario rupture.

2.2 COMPUTING HYBRID SEISMOGRAMS

To compute the seismograms we employ the discrete wavenumber code from Bouchon (1981) to model the long period component of the seismograms as well as realistic phase arrivals. For the short period component we employ the stochastic approach developed by Boore (1983) for point sources and subsequently developed for finite fault models (Motazedian and Atkinson (2005)). The seismograms are stacked in time following application of a matching pair of filters.

2.2.1 Stochastic approach for frequencies above 1Hz

To model synthetic seismograms and the corresponding response spectra, we employ the EXSIM code developed by Motazedian and Atkinson (2005). EXSIM is a finite fault stochastic modelling code that takes into account source as well as regional parameters, and generates realistic broadband seismograms. In the stochastic approach, the moment of the modelled earthquake controls the low-frequency part of the spectra, whereas the stress drop controls the high-frequency part. The stochastic code is advantageous as it is fast and efficient in the frequency range above 1 Hz.

Exsim requires well-defined source and attenuation models. Key regional parameters used to guide the ground motion modelling have been derived using spectral inversion of the extensive Canterbury strong motion dataset (Oth & Kaiser 2013; Kaiser et al. 2013). These include: 1) a Canterbury regional frequency-dependent attenuation relationship (Kaiser et al. (in prep)); 2) stress drop estimates for each source (specifically defined for this study); and 3) site-specific horizontal and vertical frequency-dependent amplification functions (Kaiser et al. 2013). The selected site-amplification function used in this study is described in section 2.3.

2.2.2 Discrete wavenumber approach for frequencies lower than 1Hz

We compute the low frequency part of seismograms (<1 Hz) using a simple elastic wave-propagation code, the Discrete Wavenumber code from Bouchon (1981). The 1D velocity model is equivalent to a flat layered structure. This approach works well for generating ground motions at those frequencies (Hartzell et al. 1999). It also allows us to include realistic phase arrivals. The regional velocity model employed in this study is the same throughout computations: a simple 1D layered velocity model from Reyners and Cowan (1993). The low-frequency and the high-frequency parts of the computed ground motions are combined together using a set of appropriate filters.

2.3 SITE EFFECTS

To start, we model standard rock-site ground motions i.e. without site effects. We do so by adopting the horizontal and vertical site-amplification functions for rock site D14C (Kaiser et al. 2013), which serves as an appropriate rock reference station (see also Van Houtte et al. 2012). In a second stage, we compute site-specific ground motions by adopting the relevant average elastic site-amplification function derived for the relevant Site Class under linear soil behaviour. We employ Site Class D amplification function from Kaiser et al. (in prep.) (Figure 5) which represents the average class D amplification observed in the Canterbury region.

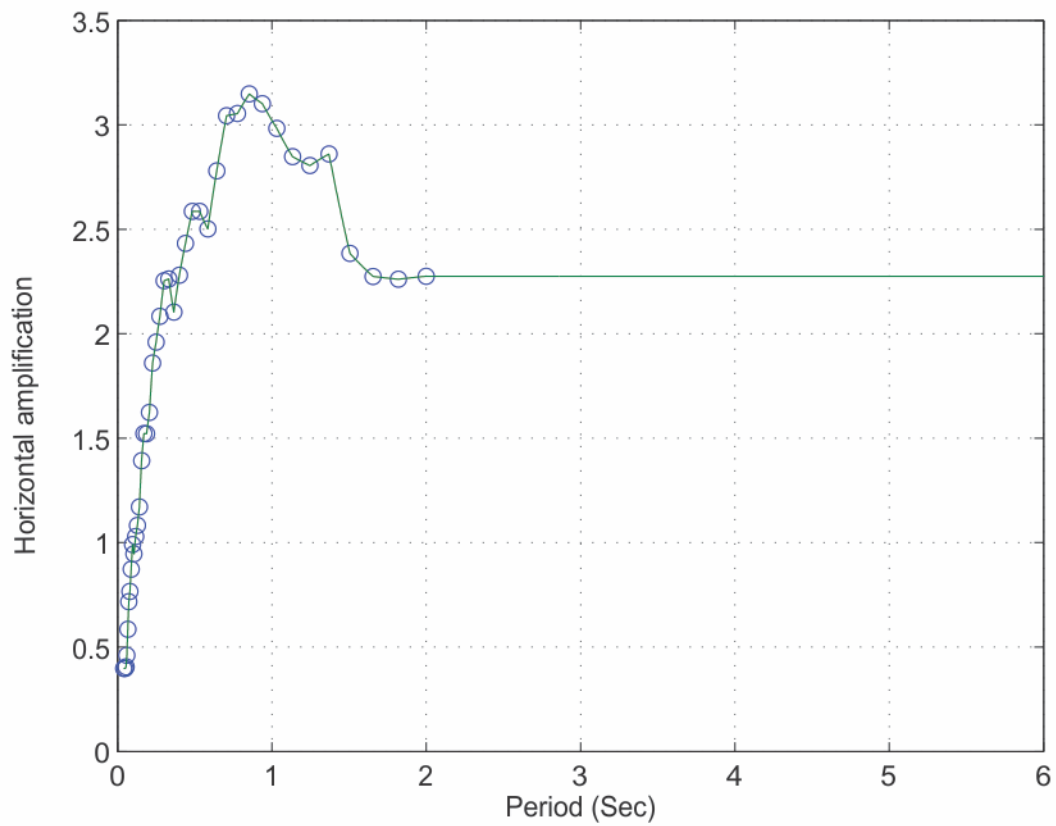


Figure 5 Horizontal amplification function for Site Class D soil type (Kaiser et al., 2014) based on the average site amplification for Class D sites in Canterbury. Values are obtained for 0.5-20Hz range and extrapolated beyond this frequency range (2 second period and longer).

3.0 CHARACTERISING A LIKELY RUPTURE SCENARIOS ON THE ALPINE FAULT

We need to quantify potential rupture areas which can be described as outer, inner and extra parameters. The parameters used in Holden and Zhao (2011) to characterise an Alpine Fault source were conservative and will be re-assessed to represent the most likely scenario rupture process for the present study.

The Alpine Fault in New Zealand is a major dextral-reverse fault that has produced large earthquakes (c. $M_w=7.9$) every 200–400 years with the last one in 1717 AD (Figure 1). In order to estimate fault-specific strong-ground motion time history, we need to quantify a potential scenario in terms of expected magnitude, length and width of the potential rupture segments, slip distribution and rupture propagation on the rupture segments. We will establish our representative models based on previous major events as shown in Figure 3 (Sutherland et al. 2007).

Sutherland et al. (2007) estimated that the previous events had a moment magnitude in the range of 7.6–7.9 for a simultaneous rupture of all fault segments which has been suggested as the most likely scenario. However, if each segment ruptures separately, then the moment magnitude of each event would be about 7.2 from an empirical relation between M_w and rupture area (Wells and Coppersmith 1994). The base of the seismogenic zone is relatively shallow. Seismicity and geodetic studies suggest a depth of 5–12 km for full fault locking (Beavan et al. 1999; Pearson et al. 2000), with a potentially deeper locking interface as deep as 18 km (Wallace et al. 2007). Each of the last two events had a maximum fault slip of 8–9 m (Sutherland et al. 2007). Rupture models for two different seismogenic rupture lengths may lead to quite different ground motion amplitudes and duration. The Alpine Fault has a strike-slip focal mechanism and an estimated dip angle of 45° . The narrow fault width and shallow dip angle for a strike-slip fault are quite unique. Broadband simulations can show some insights on how these affect the duration of the strong shaking and response spectra.

3.1 OUTER PARAMETERS

The outer parameters are the geometry of the fault plane, its dimensions, and seismic moment. The values selected for parameters depend on the modelling scenarios, here the whole Alpine Fault. The total seismogenic zone S is estimated for this particular scenario and the total moment is estimated using the following relationship (Miyake et al. 2003; Irikura and Miyake, 2006):

- $S(\text{km}^2)=5.10 \times 10^{-25} \times M_0$ for $M_0 \geq 7.5 \times 10^{27}$ dyne.cm (Scholtz 2002)

Summary:

- Magnitude M_w 8.2
- Total rupture area 6000 (500 by 12) km^2 (Scholtz 2002)
- Total Seismic Moment: 2.24×10^{21} Nm

3.2 INNER PARAMETERS

Inner parameters represent the combined asperity area on the overall fault plane as well as the corresponding stress drop. To estimate the combined asperity area, an empirical relationship (Somerville et al. 1999) suggests that 22% of the overall fault plane is composed of asperities for inland crustal earthquakes. On the other hand, Sutherland et al. (2007) suggested the presence of “low stress patches” on the fault likely to act as barriers for the rupture, but not strong enough to stop the rupture completely. In this case, the areas on the fault where no low stress patches are observed can also be considered as “asperities”. The locations of asperities may also be identified by surveys of fault displacement from past earthquakes. The location of large fault displacement at the ground surface may be the location of a fault segment that has an asperity.

We use the empirical scaling relation from Somerville et al. (1999) relating asperity area to total rupture area and the estimated asperity area is 1300 km² (around 22%). The 3 largest asperities as described in the subsequent source paragraph give an average (and rounded) asperity area of 50 by 10 km².

We distributed the asperities at locations where very large coseismic ground displacements have been observed in previous events (Figure 3). The southern-most asperity in this model (ASP2) is located onshore, near Milford Sound (MSZ), the second asperity (ASP3) is located near Jackson Bay (JCZ) and the third asperity (ASP4) is located at the northern part of the fault (WVZ), 150 km away from Christchurch. Descriptions of the asperities are summarized in Table 2 and Figure 6.

Stress drop for each asperity is based on the value obtained from modelling the recent 2008 Mw 7.9 Wenchuan crustal event (Kurahashi and Irikura, 2010). They calculated a stress drop value of 13.6 MPa for asperities with analogous rupture areas. This value is very high but only relates to the asperity area, not the overall rupture.

Table 2 Source characteristics of the main event and the 3 modelled asperities for an Mw 8.2 Alpine fault characterized source model. The rupture times are based on the assumption of a unilateral South to North rupture with a 2.5 km/s rupture velocity.

	Size (LxW)(km ²)	Moment (Nm)	Mw	Stress drop (MPa)	Distance from ASP2 (km)	Rupture time (sec)
Main Event	500x18	2.24 x10 ²¹	8.2			
ASP2	50x10	1.35x10 ²⁰	7.4	13.6	0	0
ASP3	50x10	1.35x10 ²⁰	7.4	13.6	100	40
ASP4	50x10	1.35x10 ²⁰	7.4	13.6	300	120



Figure 6 Characterized source model for a Mw 8.2 Alpine fault rupture; the model consists of a background area (blue) of 500 by 18 km and 3 asperity areas of 50 by 10 km each. Note the dimensions along strike and along depth are not to scale.

3.3 EXTRA PARAMETERS

Nucleation and termination of the rupture represent the extra parameters related to the propagation pattern. Geodetic and seismicity studies suggest that the Alpine Fault is locked in its central part from Haast to Tamarakau River (Sutherland et al. 2007). This is where the nucleation of a major event is most likely to occur. Their modelling results also suggest that an episode of aseismic slip at depth may inhibit the nucleation of an event above it but will not stop the rupture propagation. Therefore detailed characterisation of the structure at depth will help constrain potential locations for an event nucleation.

Initiation of the rupture is likely at the southern end of the Alpine fault, based on the fact that this is where the fault is most strongly coupled. We are therefore modelling a South to North rupture. For every site, ground motion resulting from the rupture of each asperity is stacked in time according to their respective rupture time and an arbitrary chosen rupture velocity of 2.5 km/s (Table 2).

4.0 CHARACTERISING A LIKELY RUPTURE SCENARIO ON THE HOPE FAULT

The following parameters have been estimated from the same process as described in the previous section for the Alpine Fault.

4.1 OUTER PARAMETERS

The Hope Fault is a dextral fault extending northeast from the Alpine Fault (Figure 1). The last rupture of the Hope Fault was in 1888 when an earthquake with an estimated moment magnitude of 7-7.3 produced a fault slip of about 2.5 m in the horizontal direction. Our modelling will be based on this event. Following Cowan (1991) and recent re-interpretation of the rupture features (R. Langridge, GNS Science, pers. Com.), we estimate the rupture dimensions of the modelled event to be 45 km in strike by 13 km in depth (Figure 4). The strike and dip of the fault are 260 degrees and 80 degrees respectively and the fault rupture is right-lateral.

4.2 INNER PARAMETERS

We used the empirical scaling relation from Somerville et al. (1999) relating asperity area to total rupture area and the estimated asperity area is 120 km² (around 22%). Following the recipe, we infer the occurrence of one asperity for an M 7.1 Hope fault rupture. The average asperity area is 120km². Considering a rather shallow seismogenic depth of 13 km, we define the asperity area dimensions as 12 km along the strike and 10 km in depth.

We located the asperity where very large coseismic ground displacements have been observed in the previous events (Figure 3), about 10 km north of the Hope and Kiwi river confluence that characterises the southernmost tip of our modelled rupture (Figure 7).

The stress drop value for the asperity of 10 MPa is a compromise between the value of 13.6 MPa obtained from modelling the recent 2008 Mw 7.9 Wenchuan crustal event (Kurahashi and Irikura, 2010) and the recent value obtained for the Mw 6.2 Christchurch earthquake of 9.2 MPa (Oth and Kaiser (2013)). As in the Alpine Fault case study, this value is very high but only relates to the asperity area, not the overall rupture.

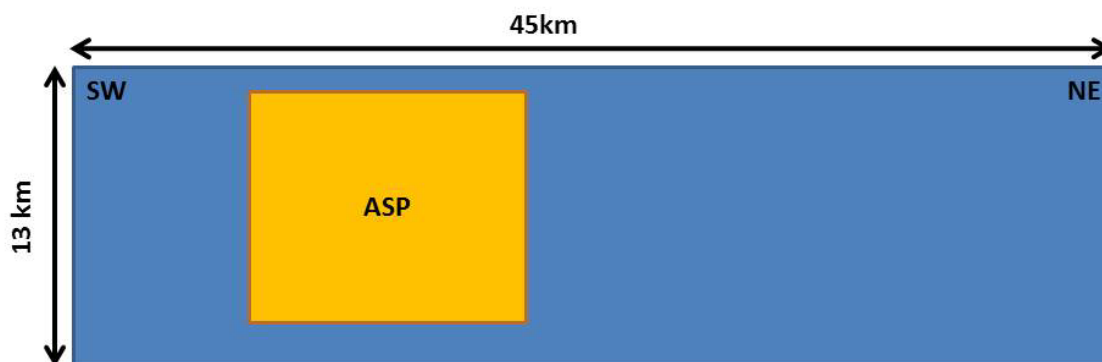


Figure 7 Characterized source model for an Mw 7.1 Hope Fault rupture; the model consists of a background area (blue) of 45 by 13 km and 1 asperity of 12 by 10 km each. The dimensions along strike and dip are to scale.

Table 3 Source characteristics of the main event and the modelled asperity for an Mw 7.1 Hope fault characterized source model.

	Size (LxW)(km ²)	Moment (Nm)	Mw	Stress drop (MPa)
Main Event	45x13	5.49 x10 ¹⁹	7.1	
ASP1	12x10	2.77x10 ¹⁹	6.9	10

4.3 EXTRA PARAMETERS

From Cowan (1991), we infer a rupture direction from Southwest to Northeast. Hence we place the hypocentre of the modelled rupture in the southwest region of the fault plane.

5.0 ACCELERATION TIME HISTORIES AND RESPONSE SPECTRA FROM AN ALPINE FAULT EARTHQUAKE

We computed acceleration time histories and the corresponding response spectra at three selected locations, based on a characterised source model of a potential Alpine Fault rupture and using a hybrid computing approach. Results are presented in the following sections.

5.1 ACCELERATION TIME HISTORIES

Figure 8 and Figure 9 show synthetic acceleration time histories at the selected rock sites and class D soil sites, respectively. For rock sites, the peak ground accelerations (PGA) of 0.16, 0.41 and 0.05g were estimated for Greymouth, Hokitika and Christchurch, respectively. For soft soil sites, the PGA estimated is 0.24g for Greymouth, 0.59g for Hokitika and 0.08g for Christchurch. We compare these values with expected PGAs from an Alpine Fault earthquake using the McVerry et al. (2006) GMPE in Table 4. The PGA values from the McVerry et al. (2006) model are in agreement for Greymouth and Christchurch (within 0.05g). However the broadband modelling for Hokitika predicts over twice the PGA from the McVerry et al. (2006) model. This difference is likely a result of our linear soil response modelling and the proximity to Hokitika of one of the modelled asperities.

Shaking duration exceeds 3 minutes at all sites. The selected sites are all located at the northern part of the fault rupture, and the chosen rupture direction would lead to strong directivity effect (“shorter” durations and large amplitudes). However, if the earthquake were to rupture from north to south, shaking intensities are expected to be less and the duration is likely to increase.

A separate study from Holden and Zhao (2011) was based on a very conservative source model of the Alpine Fault rupture with 4 asperities. Holden and Zhao (2011) simulations were built entirely on empirical Green’s function approach and local site amplification was modelled deterministically using a 1-D equivalent linear model for a representative site in Christchurch. However their results are nonetheless very similar to this study with an estimated horizontal PGA of 0.04g.

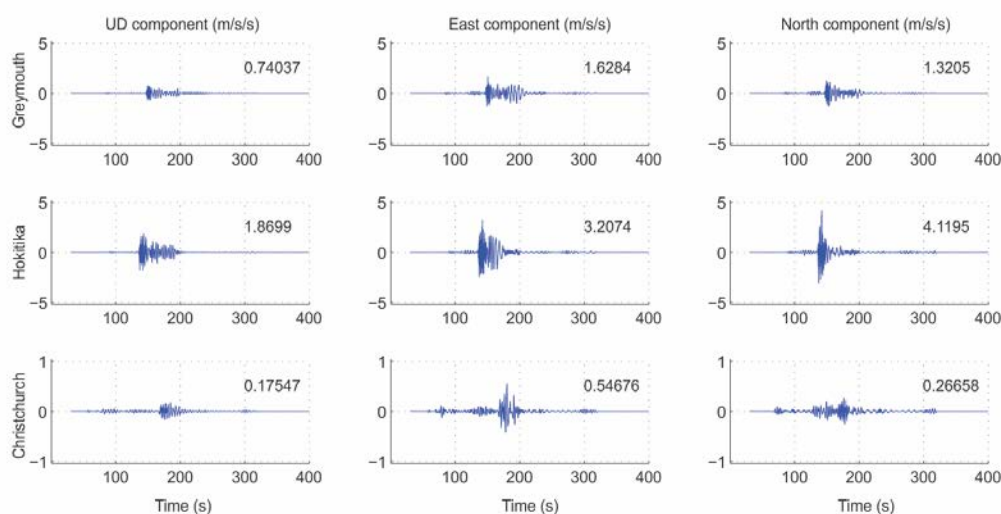


Figure 8 Horizontal and vertical synthetic acceleration histories for rock sites as modelled from a Mw 8.2 Alpine fault earthquake in Greymouth, Hokitika and Christchurch (top to bottom). The number above each trace represents PGA in m/s/s.

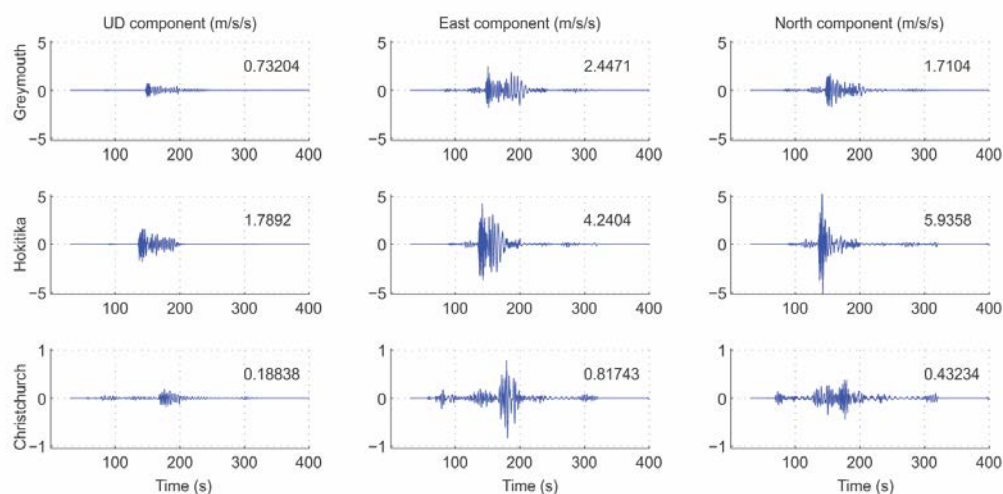


Figure 9 Horizontal and vertical synthetic acceleration histories for a Site Class D site as modelled from a Mw 8.2 Alpine fault earthquake in Greymouth, Hokitika and Christchurch (top to bottom). The number above each trace represents PGA in m/s/s.

Table 4 Peak ground acceleration values from the broadband modelling in this study (left column) and the McVerry et al. (2006) model (GMPE) (right column) for an Alpine fault earthquake at selected locations.

	PGA (m/s/s)	PGA McVerry (2006)(m/s/s)
Greymouth	2.4	2.0
Hokitika	5.9	2.7
Christchurch	0.8	0.6

5.2 RESPONSE SPECTRA

We calculated 5% damped acceleration spectra from the synthetic acceleration time histories. We also compare these values with expected response spectra from an Alpine Fault earthquake using the McVerry et al. (2006) GMPE via openSHA (Field et al., 2003). Figure 10 shows synthetic response spectra for rock conditions (blue), soft soil conditions (red) and the GMPE model (McVerry et al., 2006) (green) for the horizontal components.

For Greymouth and Christchurch, the deterministic synthetic spectra are in agreement with the GMPE model for the short periods (up to 0.2 sec). For periods between 0.2 and 2 seconds the deterministic spectra are much lower than the values from the GMPE model. However for spectral periods over 2 seconds, the deterministic models are much larger than the values from the GMPE model. For Hokitika, the spectra from the deterministic models are much larger than the spectrum from the GMPE models at all spectral periods within 2s.

The lack of energy in the simulated 5% damped acceleration response spectra around the 1 second period can be due to computational and natural causes. The technique employed in this study uses a matched pair of filters at 1 second period. Although the filters are carefully selected, some loss of energy at about that period is possible. Response spectra have also a natural variability. Simulations from Holden and Zhao (2011) based entirely on broadband empirical Green's functions also show a deficiency in the responses at about 1 second period. The response spectra computed from data recorded at the GeoNet station CECS during the Mw 7.1 2010 Darfield earthquake also show a natural deficiency in spectral acceleration at about 1 second period (Figure 2).

Because of the very limited records from large earthquakes used in dataset of the McVerry et al. (2006) study, we do not expect that the GMPE would predict the long period spectrum from large events very well. For spectral periods over 3s, the McVerry et al. (2006) model used an assumption of constant displacement spectrum while the NGA models by Abrahamson and Silva (2008) employed an assumption of constant displacement spectrum at a much longer spectral period than 3s. Therefore it is not surprised that the spectra from the broadband simulations are larger than those from the GMPE models by McVerry et al. (2006) for the long period part of the spectra.

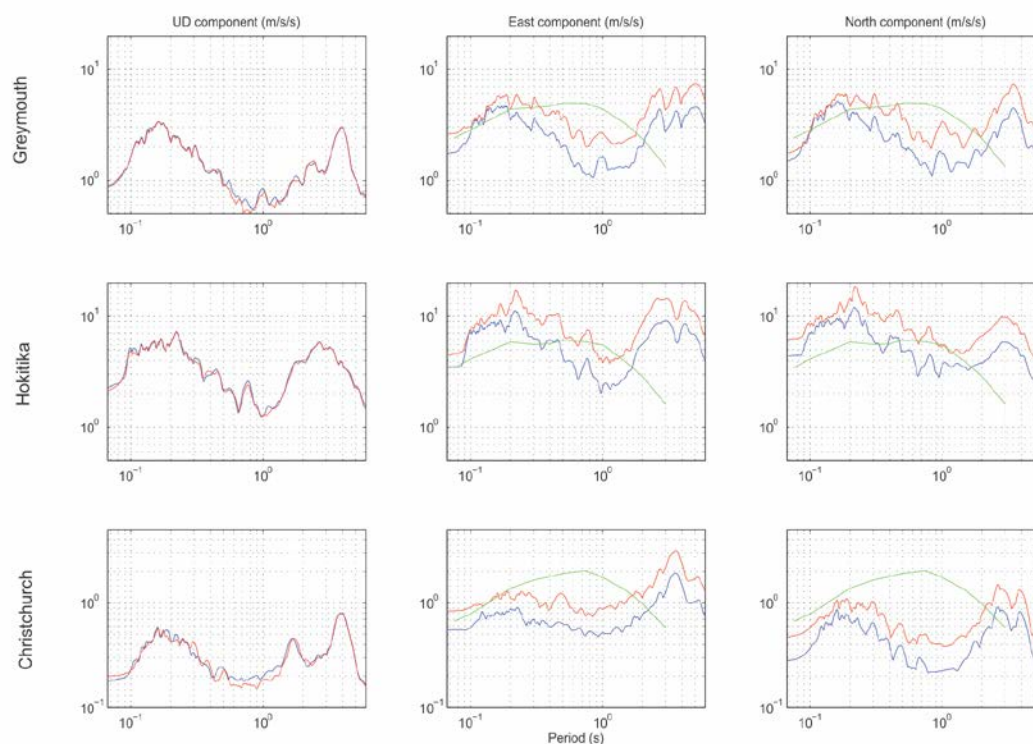


Figure 10 Horizontal and vertical response spectra (5% damped) for rock sites (blue), Site Class D (red) soil sites as modelled from a Mw 8.2 Alpine Fault earthquake in Greymouth, Hokitika and Christchurch (top to bottom). The green line represents the response spectra obtained from the McVerry et al. (2006) GMPE.

6.0 ACCELERATION TIME HISTORIES AND RESPONSE SPECTRA FROM A HOPE FAULT EARTHQUAKE

We computed acceleration time histories and the response spectra at three selected locations, based on a characterised source model of a potential Hope fault rupture, using a hybrid approach. Results are presented in the following sections.

6.1 ACCELERATION TIME HISTORIES

Figure 11 and Figure 12 show synthetic acceleration time histories at selected rock sites and Site Class D soil sites respectively. For the rock sites, the estimated PGA is 0.08g for Greymouth, 0.03g for Hokitika and 0.06g for Christchurch. For soft sites, the estimated PGA is 0.11g for Greymouth, 0.05g for Hokitika and 0.08g for Christchurch. Table 5 compares these values with the estimated PGAs from a Hope Fault earthquake using the GMPE by McVerry et al. (2006). PGA values from the McVerry et al. (2006) model are in good agreement for all sites, with the largest difference of 0.03g. This level of shaking is similar to recordings at GeoNet strong motion stations, KOKS and CECS (Figure 1), located similar distances (112 and 120 km respectively) from the epicentre of the 2010 Mw 7.1 Darfield earthquake with PGAs ranging between 0.03-0.05g.

Shaking duration at all three modelled sites is expected to be about 20 seconds. However this is a lower band value since the modelling presented in this report does not include features such as basin effects and source complexities that may increase the duration of strong ground shaking.

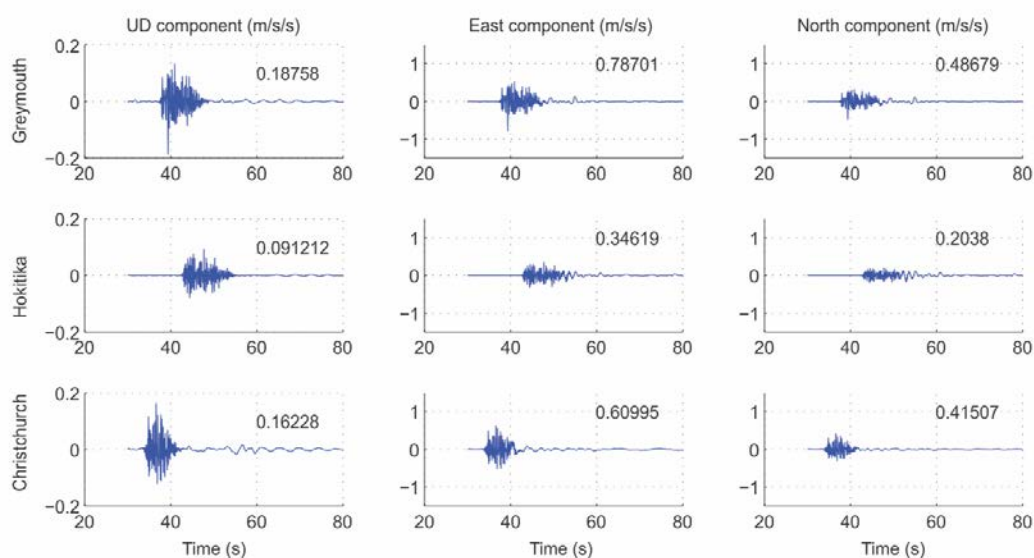


Figure 11 Horizontal and vertical synthetic acceleration histories for rock sites as modelled from a Mw 7.1 Hope fault earthquake in Greymouth, Hokitika and Christchurch (top to bottom). The number above each trace represents PGA in m/s/s.

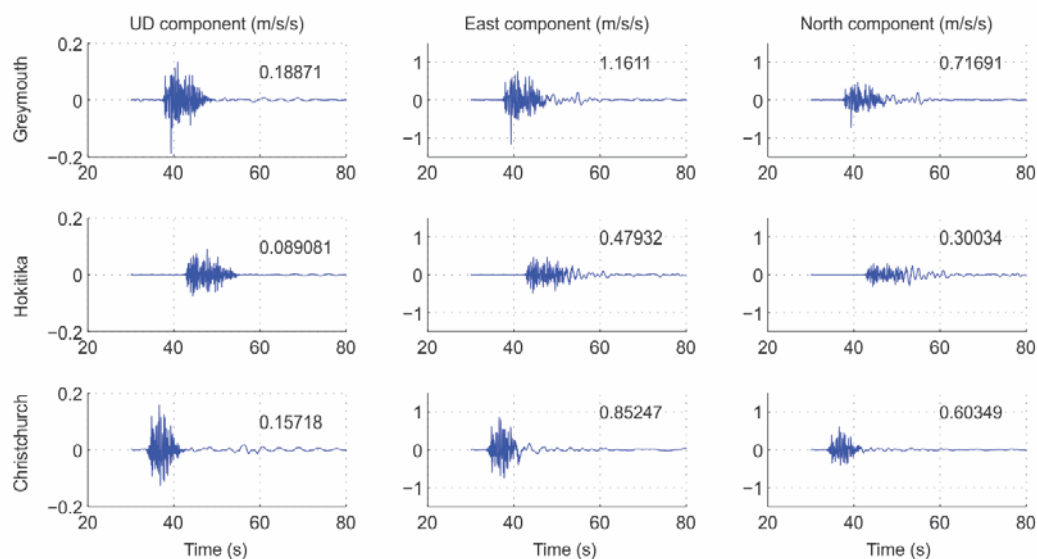


Figure 12 Horizontal and vertical synthetic acceleration histories for Site Class D soil sites as modelled from a Mw 7.1 Hope fault earthquake in Greymouth, Hokitika and Christchurch (top to bottom). The number above each trace represents PGA in m/s/s.

Table 5 Peak ground acceleration values from broadband modelling in this study (left column) and the McVerry et al. (2006) model (GMPE) (right column) for a Hope Fault earthquake at selected locations.

	PGA (m/s/s)	GMPE PGA (m/s/s)
Greymouth	0.8	0.5
Hokitika	0.3	0.4
Christchurch	0.6	0.5

6.2 RESPONSE SPECTRA

We calculated the 5% damped acceleration spectra from the synthetic acceleration time histories. Figure 13 compares the response spectra from the synthetic records (blue and red) with those (green) estimated by the McVerry et al (2006) model (Site Class D) for a Hope Fault earthquake. The response spectra from the simulations exceed the response spectra from GMPE at many spectral periods except for those between 0.7 and 0.9 second, and except for the North component of the Christchurch site where the simulations underpredict spectral accelerations for periods from 0.5 seconds and longer.

The lack of energy in the simulated 5% damped acceleration response spectra around the 1 second period can be due to computational and natural causes. This is explained in more details in section 5.2. The synthetic response spectra at all sites are very similar to the response spectra computed from data recorded at the GeoNet station CECS during the Mw 7.1 2010 Darfield earthquake, similarly showing a natural deficiency at about 1 second period (Figure 2).

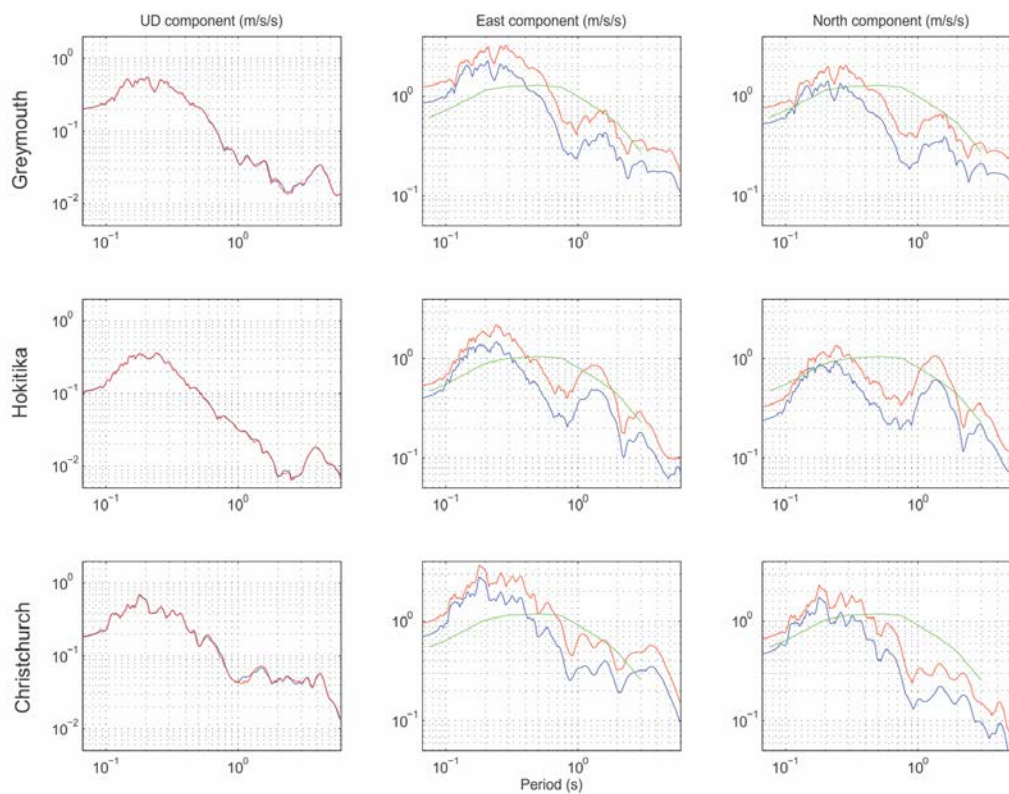


Figure 13 Horizontal and vertical response spectra (5% damped factor) for rock sites (blue), Site Class D (red) soil sites as modelled from a Mw 7.1 Hope fault earthquake in Greymouth, Hokitika and Christchurch (top to bottom). The green line represents the response spectra obtained from the McVerry et al. (2006) GMPE (Site Class D).

7.0 OUTCOMES OF THIS RESEARCH PROJECT

This report presents the broadband synthetic strong-ground motions for potential major earthquake scenarios on the Alpine Fault and the Hope Fault. Synthetic strong-motion time histories are computed for three population centres in the South Island, incorporating effects such as the location of asperities, forward directivity, site effects, and appropriate durations of strong ground shaking. Major outcomes of this study are:

- Broadband time histories at rock sites for each of the three population centres;
- Broadband time histories for soil sites derived by using empirically constructed linear site amplification ratios;
- Engineering parameters for the synthetic ground motions including response spectra, peak ground acceleration and appropriate duration of strong ground shaking.

This study presents the estimated ground motions at key locations based on given scenarios, simple source assumptions and simple ground motion modelling techniques. The approach employed in this study is intended to be timely efficient, but comprehensive in details by including reasonable source assumptions, validated computing methods and reasonable site responses. The approach however includes some limitations. These include the use of a simple 1D velocity model. Future modelling including a recently compiled 3D velocity structure for Canterbury (Lee et al., 2014) will allow for more realistic modelling of basin effects and shaking duration. Furthermore the assumed site response function is for linear motion, which may lead to an overestimation of PGAs for the strongest shaking modelled in our scenarios. Finally, this study focuses on given scenarios that were defined following reasonable assumptions. However future simulations should consider a broader range of source parameters such as variable rupture lengths and geometries, a range of asperity locations and diverse stress drop values.

8.0 ACKNOWLEDGEMENTS

The author would like to thank Kelvin Berryman, Rob Langridge and Haruko Sekiguchi for fruitful discussions. In particular, Rob Langridge's input into characterization of the Hope fault was extremely valuable. The author also acknowledges Anna Kaiser and John Zhao for reviewing this manuscript.

9.0 REFERENCES

- Aagaard, B., C. A. Williams, and B. Fry, Factors Contributing to Multi-Fault Rupture in the 2010 M7.1 Darfield, New Zealand, Earthquake, AGU Fall Meeting, 2012.
- Beavan, J.; Moore, M.; Pearson, C.; Henderson, M.; Parsons, B.; Bourne, S.; England, P.; Walcott, R.I.; Blick, G.; Darby, D.; Hodgkinson, K. 1999 Crustal deformation during 1994-98 due to oblique continental collision in the central Southern Alps, New Zealand, and implications for seismic potential of the Alpine fault. *Journal of Geophysical Research*, 104(B11): 25233-25255.
- Benites, R.A.; Olsen, K.B. 2005. Modeling strong ground motion in the Wellington metropolitan area, New Zealand. *Bulletin of the Seismological Society of America*, 95, 2180-2196.
- Boore, M.D. 1983 Stochastic simulation of high-frequency ground motions based on seismological models of the radiated spectra. *Bulletin of the Seismological Society of America*, 73: 1865–1894
- Bouchon, M. 1981 A simple method to calculate Green's functions for elastic layered media *Bulletin of the Seismological Society of America* 08/1981; 71:959-971
- Bradley, B.A. (2013) A New Zealand-specific pseudospectral acceleration ground-motion prediction equation for active shallow crustal earthquakes based on foreign models. *Bulletin of the Seismological Society of America* 103(3): 1801-1822. <http://dx.doi.org/10.1785/0120120021>
- Bradley BA, Graves RW. (2014) Low frequency ($f \leq 1$ Hz) ground motion simulations of 10 events in the 2010-2011 Canterbury earthquake sequence. Palm Springs, California: Southern California Earthquake Centre (SCEC) Annual Meeting, 7-10 September 2014.
- Cowan, H.A.; McGlone M.S. (1991). "Late Holocene displacements and characteristic earthquakes on the Hope River segment of the Hope Fault, New Zealand". *Journal of the Royal Society of New Zealand* 21 (4)
- Field, E. H., Jordan, T. H. and Cornell, C. A. (2003) OpenSHA: A Developing Community-Modelling Environment for Seismic Hazard Analysis. *Seismological Research Letters*, 74: 406-419.
- Hartzell, S.; Harmsen, S.; Frankel, A.; Larsen, S. 1999 Calculation of broadband time histories of ground motion: Comparison of methods and validation using strong-ground motion from the 1994 Northridge earthquake, *Bulletin of the Seismological Society of America*, 89(6): 1484-1504
- Holden, C.; Kaiser, A.E.; Massey, C.I. 2014 Broadband ground motion modelling of the largest M5.9+ aftershocks of the Canterbury 2010-2011 earthquake sequence for seismic slope response studies. Lower Hutt, NZ: GNS Science. GNS Science report 2014/13. 48 p.
- Holden, C.; Zhao, J. 2011 Preliminary broadband modelling of an Alpine fault earthquake in Christchurch. GNS Science Report 2011/28. 17 p.
- Irikura, K.; Miyake, H. 2006 Recipe for predicting strong ground motions: the state of the art and future prospects. Proceedings of the 8th U.S. National Conference on Earthquake Engineering April 18-22, 2006, San Francisco, California, USA, paper No 744
- Irikura, K.; Miyake, H. 2011 Recipe for predicting strong ground motion from crustal earthquake scenarios. *Pure Applied Geophysics*, 168: 85-104 doi:10.1007/s00024-010-0150-9.

- Kaiser A.E.; Oth A, Benites RA. Source, path and site effects influencing ground motions during the Canterbury earthquake sequence, determined from spectral inversions. Paper 18: Proceedings of the New Zealand Society for Earthquake Engineering Annual Meeting, 26 – 28 April, Wellington, 2013.
- Kaiser, A.E.; Oth, A., Benites, R.A., The role of frequency-dependent attenuation and site amplification during the Canterbury earthquake sequence, New Zealand, from spectral inversion of strong motion data. In preparation for *Geophysical Journal International*.
- Kamae, K.; Irikura, K.; Pitarka, A. 1998 A technique for simulating strong ground motion using hybrid Green's function. *Bulletin of the Seismological Society of America*, 88: 357-367
- Kurahashi, S.; Irikura, K. 2010 Characterized source model for simulating strong ground motions during the 2008 Wenchuan earthquake. *Bulletin of the Seismological Society of America*, 100(5B): 2450-2475.
- Langridge, R.M.; Campbell, J.; Hill, N.L.; Pere, V.; Pope, J.; Pettinga, J.; Estrada, B.; Berryman, K.R. 2003 Paleoseismology and slip rate of the Conway Segment of the Hope Fault at Greenburn Stream, South Island, New Zealand. *Annals of Geophysics*, 46(5): 1119-1139
- Lee, R.L., Bradley, B.A., Pettinga, J., Hughes, M. and Graves, R.W. (2014) Ongoing development of a 3D seismic velocity model for Canterbury, New Zealand for broadband ground motion simulation. Auckland, New Zealand: 2014 New Zealand Society for Earthquake Engineering Annual Conference (NZSEE), 21-23 Mar 2014. 8pp.
- Mai, P.M.; Imperatori, W.; Olsen, K.B. 2010. Hybrid broadband ground-motion simulations: Combining long-period deterministic synthetics with high-frequency multiple S-to-S backscattering. *Bulletin of the Seismological Society of America*, 100, 2124-2142.
- McVerry, G.H.; Zhao, J.X.; Abrahamson, N.A.; Somerville, P.G. 2006 New Zealand acceleration response spectrum attenuation relations for crustal and subduction zone earthquakes. *Bulletin of the New Zealand Society for Earthquake Engineering*, 39(1): 1-58
- Miyake, H.; Iwata, T.; Irikura, K. 2003 Source characterization for broadband ground-motion simulation: Kinematic heterogeneous source model and strong motion generation area. *Bulletin of the Seismological Society of America*, 93: 2531-2545.
- Oth, A.; Kaiser, A.E. 2013 Stress release and source scaling of the 2010-2011 Canterbury, New Zealand earthquake sequence from spectral inversion of ground motion data. *Pure and Applied Geophysics*, Online first: doi: 10.1007/s00024-013-0751-1 (16 p.)
- Pearson, C.; Denys, P.; Hodgkinson, K. 2000 Geodetic constraints on the kinematics of the Alpine Fault in the southern South Island of New Zealand, using results from the Hawea-Haast GPS transect. *Geophysical Research Letters*, 27(9): 1319-1322.
- Pulido N.; Kubo, T. 2004 Near-Fault Strong Motion Complexity of the 2000 Tottori Earthquake (Japan) from a Broadband Source Asperity Model. *Tectonophysics*, 390: 177-192.
- Reyners, M.E.; Cowan, H. 1993 The transition from subduction to continental collision : crustal structure in the North Canterbury region, New Zealand. *Geophysical Journal International*, 115(3): 1124-1136
- Somerville, P.; Irikura, K.; Graves, R.; Sawada, S.; Wald, D.; Abrahamson, N.; Iwasaki, Y.; Kagawa, T.; Smith, N.; Kowada, A. 1999 Characterizing crustal earthquake slip models for the prediction of strong ground motion. *Seismological Research Letters*, 70(1): 59-80.

- Sutherland, R.; Eberhart-Phillips, D.; Harris, R.A.; Stern, T.A.; Beavan, R.J.; Ellis, S.M.; Henrys, S.A.; Cox, S.C.; Norris, R.J.; Berryman, K.R.; Townend, J.; Bannister, S.C.; Pettinga, J.; Leitner, B.; Wallace, L.M.; Little, T.A.; Cooper, A.F.; Yetton, M.; Stirling, M.W. 2007 Do great earthquakes occur on the Alpine Fault in central South Island, New Zealand? p. 235-251 IN: Okaya, D.A.; Stern, T.A.; Davey, F.J. (eds) A continental plate boundary: tectonics at South Island, New Zealand. Washington, DC. American Geophysical Union. Geophysical monograph 175.
- Van Houtte, C., Ktenidou, O.-J., Larkin, T., Kaiser, A. 2012. Reference stations for Christchurch. Bulletin of the New Zealand Society for Earthquake Engineering, Vol 45(4): 184-195. Wallace, L.M.; Beavan, J.; McCaffrey, R.; Berryman, K.; Denys, P.; 2007 Balancing the plate motion budget in the South Island, New Zealand, using GPS, geological and seismological data. Geophysical Journal International, 168(1): 332-352.
- Wells, D.L.; Coppersmith, K.J. 1994 New empirical relationships among magnitude, rupture length, rupture width, rupture area, and surface displacement. Bulletin of the Seismological Society of America, 84(4): 974-1002
- Yetton, M.D. 2000 The probability and consequences of the next Alpine fault earthquake, South Island, New Zealand. PhD thesis, Department of Geological Sciences, University of Canterbury, New Zealand.
- Zhao, J.X.; Lu, M. 2011 Magnitude-scaling rate in ground-motion prediction equations for response spectra from large shallow crustal earthquakes. Bulletin of the Seismological Society of America, 101(6): 2643-2661
- Zhao, J.X. and Xu 2012 Magnitude-scaling rate in ground-motion prediction equations for response spectra from large subduction interface earthquakes in Japan. Bulletin of the Seismological Society of America, 102(1), 222-235



www.gns.cri.nz

Principal Location

1 Fairway Drive
Avalon
PO Box 30368
Lower Hutt
New Zealand
T +64-4-570 1444
F +64-4-570 4600

Other Locations

Dunedin Research Centre
764 Cumberland Street
Private Bag 1930
Dunedin
New Zealand
T +64-3-477 4050
F +64-3-477 5232

Wairakei Research Centre
114 Karetoto Road
Wairakei
Private Bag 2000, Taupo
New Zealand
T +64-7-374 8211
F +64-7-374 8199

National Isotope Centre
30 Gracefield Road
PO Box 31312
Lower Hutt
New Zealand
T +64-4-570 1444
F +64-4-570 4657